



Shear correction factors for functionally graded plates

T. K. Nguyen, Karam Sab, Guy Bonnet

► To cite this version:

T. K. Nguyen, Karam Sab, Guy Bonnet. Shear correction factors for functionally graded plates. *Mechanics of Advanced Materials and Structures*, 2007, 14 (8), pp.567-575. 10.1080/15376490701672575 . hal-00691061

HAL Id: hal-00691061

<https://hal.science/hal-00691061>

Submitted on 16 Jan 2016

HAL is a multi-disciplinary open access archive for the deposit and dissemination of scientific research documents, whether they are published or not. The documents may come from teaching and research institutions in France or abroad, or from public or private research centers.

L'archive ouverte pluridisciplinaire **HAL**, est destinée au dépôt et à la diffusion de documents scientifiques de niveau recherche, publiés ou non, émanant des établissements d'enseignement et de recherche français ou étrangers, des laboratoires publics ou privés.

Shear Correction Factors for Functionally Graded Plates

T.-K. Nguyen and K. Sab

Université Paris-Est, Institut Navier, LAMI (ENPC/LCPC), France

G. Bonnet

Université Paris-Est, Laboratoire de Mécanique (EA 2545), Institut Navier, UMLV, France

The Reissner-Mindlin plate model for calculation of functionally graded materials has been proposed in literature by using shear correction coefficient of homogeneous model. However, this use is a priori not appropriate for the gradient material. Identification of the transverse shear factors is thus investigated in this paper. The transverse shear stresses are derived by using energy considerations from the expression of membrane stresses. Using the obtained transverse shear factor, a numerical analysis is performed on a simply supported FG square plate whose elastic properties are isotropic at each point and vary through the thickness according to a power law distribution. The numerical results of a static analysis are compared with available solutions from previous studies.

Keywords functionally graded materials, elasticity, plates, shear correction factors

1. INTRODUCTION

Multilayered materials are used in many structures of mechanical engineering and civil engineering. In conventional laminated composite structures, homogeneous elastic laminae are bonded together to obtain enhanced mechanical and thermal properties. The main inconvenience of such an assembly is that they create stress concentrations along the interfaces, more specifically when high temperatures are involved. This can lead to delaminations, crackings, and other damage mechanisms which result from the abrupt change of the mechanical properties at the interface between the layers. One way to overcome this problem is to use functionally graded materials within which material properties vary continuously. The concept of functionally graded material (FGM) was proposed in 1984 by the material scientists in the Sendai area of Japan [1]. The FGM is a composite whose composition varies according to the required performance. It can be produced with a continuously graded variation of the volume fractions of the constituents. That leads to a continuous change of the material properties of FGM, which

is the main difference between such a material and an usual composite material. The FGM is suitable for various applications, such as thermal coatings of barrier for ceramic engines, gas turbines, nuclear fusions, optical thin layers, biomaterial electronics, etc. Its applications within several fields requires special manufacturing methods and evaluation methods [2–4].

Functionally graded (FG) plate models have been studied using analytical and numerical methods. Various approaches have been developed led to establish the appropriate analysis of the FG plates. The model based on classical plate theory (CPT) of Love-Kirchhoff was used by Chi and Chung [5, 6] for the FGM. They developed the analytical solution of simply supported FG plates subjected to mechanical loads. A finite element formulation based on the CPT was developed by He et al. [7] to control the shape and vibration of the FG plate with integrated piezoelectric sensors and actuators. In practice, this model is not used for thick plates which have an important contribution of the shear deformation energy. Several authors analyzed the behavior of thick FG plates. They proposed models that take into account the transversal shear effect, by using the First-order Shear Deformation Theory (FSDT) [8, 9] and the higher-order shear deformation theories [10, 11]. Praveen and Reddy [12] analyzed the nonlinear static and dynamic responses of functionally graded ceramic-metal plates using the first-order shear deformation theory (FSDT) and the von Karman strain (see Reddy [10, 11]). Croce and Venini [13] developed a hierarchic family of finite elements according to the Reissner-Mindlin theory. The model of FSDT plate is the simplest plate model that accounts for the transverse shear strains, which are assumed constant through the plate thickness. This model requires shear correction coefficients to compute transverse shear forces. To avoid this difficulty, several authors proposed the higher-order shear deformation theory and applied it to FGM. Reddy [14] developed the Navier's solutions for functionally graded plates using the Third-order Shear Deformation plate Theory (TSDT) and an associated finite element model. Cheng and Batra [15] also used the theory of Reddy (TSDT) for studying the buckling and steady state vibrations of a simply supported functionally graded polygonal plate. Ferreira et al. [16] have presented results from a static analysis of FG plates by using the Reddy's plate theory and a meshless method.

Received 28 March 2007; accepted 8 May 2007.

Address correspondence to G. Bonnet, LaM (Université de Marne-La-Vallée), 5 bd Descartes, 77454 Marne-La-Vallée, France. E-mail: Guy.Bonnet@univ-mlv.fr

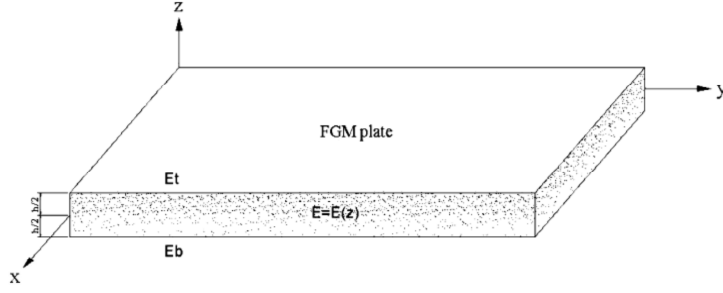


FIG. 1. Geometry of the functionally graded plate.

Moreover, the Sinusoidal Shear Deformation Theory (SSDT) of Zenkour [17, 18] was used for FG plates. By using the theory himself, Zenkour [19] presented Navier's analytical solution of FG plates. In the higher-order shear deformation theory, the transverse shear stresses are more correctly approximated throughout the thickness and consequently no transversal shear correction factors are needed. For the thick FG plates whose thickness is not negligible, when compared to the side length, the three-dimensional model for static and dynamic problem can be used. Cheng and Batra [20] studied thermomechanical deformations of the FG plates. A discrete layer approach was proposed by Ramirez [21] for the static analysis of three-dimensional FG plates.

The model based on the first-order shear deformation theory (FSDT) is very often used owing to its simplicity in analysis and programming. It requires however a correct value of the shear correction factor. In practice, this coefficient is equal to 5/6 for homogeneous plates. But, this value is a priori no longer appropriate for FG plate analyses due to the position dependence of FGM material properties. The primary objective of this paper is thus to identify the shear correction coefficients for functionally graded Reissner-Mindlin plates. The influence of this factor on the static responses of FG plate is then presented. A numerical test is performed on a simply supported FG ceramic-metal plate. The material properties are supposed to be isotropic and varying through the thickness according to a power-law distribution in terms of the volume fractions of the components.

2. THEORETICAL FORMULATION

2.1. Functionally Graded Materials

Let us consider a Reissner-Mindlin plate having a thickness h which is located within a domain $\Omega = \omega \times]-\frac{h}{2}, \frac{h}{2}[$, $h \in \mathbb{R}^+$. $\omega \in \mathbb{R}^2$ is a domain having a boundary with a suitable regularity $\partial\omega$. The top and bottom surfaces of the plate are denoted by $\Gamma^\pm = \omega \times \{\pm \frac{h}{2}\} = \{x, y \in \Omega, z = \pm \frac{h}{2}\}$. The plate is made of functionally graded materials which is constituted by a mixture of ceramic and metallic components. The material properties vary through the plate thickness according to the volume frac-

tions of the constituents. All formulations are performed under the assumption of a linear elastic behavior and small deformations of materials. The volume forces are not taken into account.

For a plate made of two constituents, effective properties of the materials by the thickness of the plate is defined by a power-law relation:

$$E(z) = V_c(z)E_t + [1 - V_c(z)]E_b \quad (1)$$

with,

$$V_c(z) = \left(\frac{z + \frac{h}{2}}{h} \right)^p \quad (2)$$

where p is a material parameter which takes on non-negative values, h plate thickness and $z \in [-h/2, h/2]$, E_t and E_b the Young's modulus at the top and bottom surface of the plate. It is well-known that such a relation is not exact and many more precise approximations may be found within the literature [2, 22–24]. The distribution of the materials under consideration

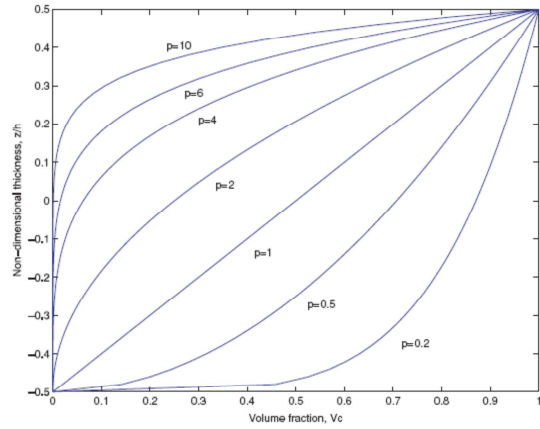


FIG. 2. Variation of V_c through plate thickness for various values of p .

through the plate thickness (2) is of the form illustrated in Figure 2, where the variation of V_c in terms of the power-law parameter is presented.

We note that the volume fraction changes rapidly near the lowest surface for $p < 1$ and increases quickly near the top surface for $p > 1$. To investigate the effect of the Poisson's ratio on the response of the plate, a variation of this ratio through the plate thickness corresponding to a similar power-law distribution will be used:

$$\nu(z) = V_c(z)\nu_t + [1 - V_c(z)]\nu_b \quad (3)$$

where ν_t and ν_b are the Poisson's ratio at the upper and lower surface of the plate.

2.2. Stress Fields

The displacement field of the first-order shear deformation theory (FSDT) and the basic equations of the Reissner-Mindlin plate can be found in [10, 11, 25]. This section presents the steps used in order to calculate shear correction factors. In the following paragraph, the Greek index is assumed to range over {1,2} while the Latin index takes {1,2,3}.

The generalized stresses associated to in-plane stress field $\sigma_{\alpha\beta}(N, M)$ can be defined as follows:

$$\begin{aligned} N_{\alpha\beta}(x, y) &= \int_{-h/2}^{h/2} \sigma_{\alpha\beta}(x, y, z) dz \\ M_{\alpha\beta}(x, y) &= \int_{-h/2}^{h/2} z \sigma_{\alpha\beta}(x, y, z) dz \end{aligned} \quad (4)$$

The generalized strains are given by,

$$\begin{aligned} \epsilon_{\alpha\beta}^o(x, y) &= \frac{1}{2}(u_{\alpha,\beta} + u_{\beta,\alpha})(x, y) \\ \chi_{\alpha\beta}(x, y) &= \frac{1}{2}(\theta_{\alpha,\beta} + \theta_{\beta,\alpha})(x, y) \end{aligned} \quad (5)$$

where the comma indicates partial differentiation with respect to the coordinate subscript that follows, u and θ the displacement and rotation of the Reissner-Mindlin model. The strain is supposed to be linear through the thickness of the FG plate,

$$\epsilon_{\alpha\beta}(x, y, z) = \epsilon_{\alpha\beta}^o(x, y) + z\chi_{\alpha\beta}(x, y) \quad (6)$$

The membrane strains and in-plane stresses are related by the constitutive equation,

$$\sigma_{\alpha\beta}(x, y, z) = C_{\alpha\beta\gamma\delta}(z)\epsilon_{\gamma\delta}(x, y, z) = C_{\alpha\beta\gamma\delta}(z)(\epsilon_{\gamma\delta}^o(x, y) + z\chi_{\gamma\delta}(x, y)) \quad (7)$$

where $C_{\alpha\beta\gamma\delta}$ are the components of the reduced stiffness tensor. By replacing eq. (7) into eq. (4), we obtain

$$\begin{aligned} N_{\alpha\beta}(x, y) &= A_{\alpha\beta\gamma\delta}\epsilon_{\gamma\delta}^o(x, y) + B_{\alpha\beta\gamma\delta}\chi_{\gamma\delta}(x, y) \\ M_{\alpha\beta}(x, y) &= B_{\alpha\beta\gamma\delta}\epsilon_{\gamma\delta}^o(x, y) + D_{\alpha\beta\gamma\delta}\chi_{\gamma\delta}(x, y) \end{aligned} \quad (8)$$

where $A_{\alpha\beta\gamma\delta}$, $B_{\alpha\beta\gamma\delta}$, $D_{\alpha\beta\gamma\delta}$ are the stiffnesses of the plate which are given by :

$$(A_{\alpha\beta\gamma\delta}, B_{\alpha\beta\gamma\delta}, D_{\alpha\beta\gamma\delta}) = \int_{-h/2}^{h/2} (1, z, z^2) C_{\alpha\beta\gamma\delta}(z) dz \quad (9)$$

Notice that, unlike a homogeneous isotropic plate where the coupling stiffnesses $B_{\alpha\beta\gamma\delta}$ do not exist, the $B_{\alpha\beta\gamma\delta}$ are present in the constitutive equation for a functionally graded plate. This arises because of material properties asymmetry about the mid-plane. The expressions of the membrane strains are finally,

$$\begin{aligned} \epsilon_{\alpha\beta}^o(x, y) &= \bar{A}_{\alpha\beta\gamma\delta}N_{\gamma\delta}(x, y) + \bar{B}_{\alpha\beta\gamma\delta}M_{\gamma\delta}(x, y) \\ \chi_{\alpha\beta}(x, y) &= \bar{B}_{\alpha\beta\gamma\delta}N_{\gamma\delta}(x, y) + \bar{D}_{\alpha\beta\gamma\delta}M_{\gamma\delta}(x, y) \end{aligned} \quad (10)$$

where $(\bar{A}, \bar{B}, \bar{D})$ are the components of the compliance matrix. Replacing Eq. (10) in Eq. (7) leads to,

$$\sigma_{\alpha\beta}(x, y, z) = n_{\alpha\beta\gamma\delta}(z)N_{\gamma\delta}(x, y) + m_{\alpha\beta\gamma\delta}(z)M_{\gamma\delta}(x, y) \quad (11)$$

where $n_{\alpha\beta\gamma\delta}(z)$, $m_{\alpha\beta\gamma\delta}(z)$ are the components of the localization tensor:

$$\begin{aligned} n_{\alpha\beta\gamma\delta}(z) &= C_{\alpha\beta\epsilon\varphi}(z)(\bar{A}_{\epsilon\varphi\gamma\delta} + z\bar{B}_{\epsilon\varphi\gamma\delta}) \\ m_{\alpha\beta\gamma\delta}(z) &= C_{\alpha\beta\epsilon\varphi}(z)(\bar{B}_{\epsilon\varphi\gamma\delta} + z\bar{D}_{\epsilon\varphi\gamma\delta}) \end{aligned} \quad (12)$$

The transverse shear stresses $\sigma_{\alpha 3}$ are obtained from the equilibrium equation and from the following conditions,

$$\begin{cases} \sigma_{ij,j} = 0, & \sigma_{zz} = 0 & \text{in } \Omega & (i, j = 1, 2, 3) \\ \sigma_{\alpha\beta}(x, y, z) = n_{\alpha\beta\gamma\delta}(z)N_{\gamma\delta}(x, y) + m_{\alpha\beta\gamma\delta}(z)M_{\gamma\delta}(x, y) \\ Q_\alpha = \int_{-h/2}^{h/2} \sigma_{\alpha 3} dz \end{cases} \quad (13)$$

The equilibrium condition in Ω enables us to determine the shear stresses $\sigma_{\alpha 3}$ from the integral:

$$\sigma_{\alpha 3} = - \int_{-h/2}^z \sigma_{\alpha\beta,\beta} d\xi \quad (14)$$

where the integration coefficients are selected to satisfy the boundary condition of the shear stresses at the upper and lower faces of the plate. By replacing Eq. (11) into Eq. (14), we obtain the following relationship

$$\sigma_{\alpha 3} = \tilde{n}_{\alpha\beta\gamma\delta}(z)N_{\gamma\delta,\beta}(x, y) + \tilde{m}_{\alpha\beta\gamma\delta}(z)M_{\gamma\delta,\beta}(x, y) \quad (15)$$

where

$$\begin{aligned} \tilde{n}_{\alpha\beta\gamma\delta}(z) &= - \int_{-h/2}^z C_{\alpha\beta\epsilon\varphi}(\xi) [\bar{A}_{\epsilon\varphi\gamma\delta} + \xi\bar{B}_{\epsilon\varphi\gamma\delta}] d\xi \\ \tilde{m}_{\alpha\beta\gamma\delta}(z) &= - \int_{-h/2}^z C_{\alpha\beta\epsilon\varphi}(\xi) [\bar{B}_{\epsilon\varphi\gamma\delta} + \xi\bar{D}_{\epsilon\varphi\gamma\delta}] d\xi \\ \tilde{n}_{\alpha\beta\gamma\delta} &= \tilde{n}_{\gamma\delta\alpha\beta} = \tilde{n}_{\beta\alpha\gamma\delta}, \quad \tilde{m}_{\alpha\beta\gamma\delta} = \tilde{m}_{\gamma\delta\alpha\beta} = \tilde{m}_{\beta\alpha\gamma\delta} \end{aligned} \quad (16)$$

For finite element models, a direct computation of the transverse stresses within Eq. (14) will require the second order derivatives of the displacement. Several authors (K. Lee [26], K.Y. Sze [27], Zenkiewicz and Zhu [28], Rolfes and Rohwer [29, 30]) used a method of postprocessing based on the three-dimensional equilibrium equations or a predictor-corrector approach or simplified assumptions. The third method [29, 30], which is used thereafter, enables the computation of shear stresses from transverse shear forces. This process allows to comply to boundary conditions involving the transverse stresses and saves an order of derivation. Other contributions on this topic for thickness plates can be found in [31, 32].

2.3. Shear Correction Factors

As known that the FSDT model requires a correct value of the shear correction factors for calculating the transversal shear forces. Several authors investigated this subject in order to improve the FSDT. Noor et al. [33–36] proposed predictor-corrector procedures to correct the shear correction factors by using iteration process. The shear correction factors obtained from this method depend on boundary conditions, plate geometry and loading conditions, and hence they cannot be directly applied for other plate configuration. Energy consideration for calculating the shear correction coefficients widely used for composite laminates can be found in [37, 38, 39]. In practice, the shear factor obtained is equal to 5/6 for isotropic homogeneous plates. But, this value is a priori no more appropriate for the FG plate analyses due to continuous variation of FGM material properties. In this paper, the shear correction factors for the FGM are obtained by comparing the strain energies of the average shear stresses with those obtained from the equilibrium (see Whitney [37], Berthelot [39], Nguyen et al. [40]). To do this, we assume a cylindrical bending around the axis y and suppress the effect of the weak terms ($N_{22,1}$ and $M_{22,1}$) on the shear stresses, that leads to

$$\sigma_{xz} = \tilde{m}_{1111}(z) Q_x \quad (17)$$

with $\tilde{m}_{1111}(z)$ defined in Eq. (16). Shear forces are related to average shear strains by the shear stiffnesses,

$$\begin{Bmatrix} Q_y \\ Q_x \end{Bmatrix} = \begin{bmatrix} H_{44} & H_{45} \\ H_{45} & H_{55} \end{bmatrix} \begin{Bmatrix} \gamma_{yz}^o \\ \gamma_{xz}^o \end{Bmatrix} \quad (18)$$

where H_{ij} ($i, j = 4, 5$) are the shear stiffnesses. For isotropic materials, there is no coupling between the shear deformations in two directions, i.e. $H_{45} = 0$ and $H_{44} = H_{55}$. Therefore, it is sufficient to identify one component H_{55} or H_{44} for the shear stiffnesses.

The shear deformation energy per unit middle surface area is thus given by the following expression:

$$\Pi_s = \frac{1}{2} Q_x^2 \int_{-h/2}^{h/2} S_{55}(z) [\tilde{m}_{1111}(z)]^2 dz \quad (19)$$

with $S_{55} = \frac{2(1+\nu(z))}{E(z)} = \frac{1}{G(z)}$, $G(z)$ is the transverse shear modulus at location z . Furthermore, the shear deformation energy per unit middle surface area is expressed by using the average shear deformation,

$$\Pi_{sm} = \frac{1}{2} Q_x \gamma_{xz}^o = \frac{1}{2} \frac{Q_x^2}{H_{55}} \quad (20)$$

The balance of the shear energy enables us to deduce,

$$H_{55} = \left(\int_{-h/2}^{h/2} S_{55}(z) [\tilde{m}_{1111}(z)]^2 dz \right)^{-1} \quad (21)$$

where H_{55} is the improved shear stiffness for FG Reissner-Mindlin plates. The shear correction coefficients are finally obtained by the following relation,

$$k_{55} = \left(\int_{-h/2}^{h/2} S_{55}(z) dz \right) H_{55} \quad (22)$$

The shear correction factors is equal to 5/6 for homogeneous plates and a priori relations Eqns. (22, 21, 16) will lead to different values for the FGM. Moreover, the use of the improved shear stiffnesses in Eq. (21) will provide a better evaluation of transverse shear forces in (18) and transverse shear stresses in Eq. (17).

3. NUMERICAL RESULTS

In this part, the effect of changing the shear correction factors on the deflection and stress of the plate will be shown. Moreover, some results for the static analysis of a simply supported square FG plate under uniformly distributed load of intensity q_o , are presented. They are compared with the third-order shear

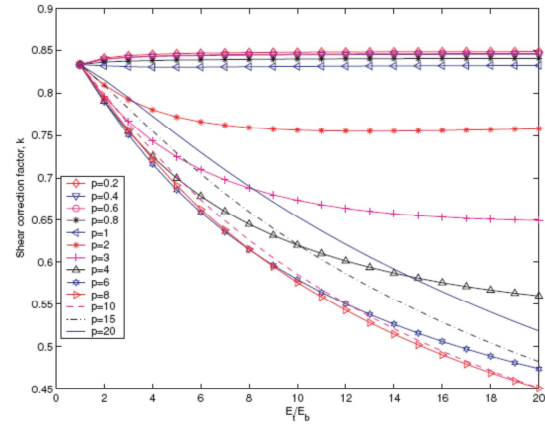


FIG. 3. Variation of the shear correction factor according to n_0 .

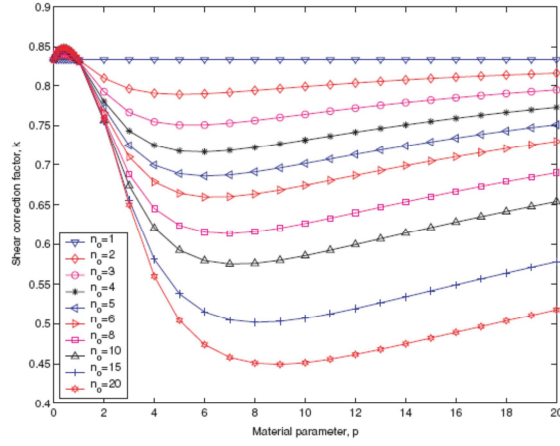


FIG. 4. Variation of the shear correction factor according to p .

deformation plate model (TSDT) of Reddy [14], the sinusoidal shear deformation plate model (SSDT) of Zenkour [19] and a discrete three-dimensional finite element model. The following parameters are used for numerical computations, $\nu = 0.3$, $a = b = 1$, $q_o = 10^4$. The Poisson's ratio is firstly supposed to be constant, we will then consider the effect of changing Poisson's ratio within the range [0.2–0.4]. The deflection and stress fields of the plate will be determined by the Navier's solution [11] and the shear stress will be calculated by the relation (17)

with the improved shear stiffnesses given in (21). The following non-dimensional parameters are used: $\bar{w} = w/h$, $\bar{\sigma} = \sigma h^2/(q_o a^2)$.

Figures 3 and 4 present the variation of the shear correction factors according to the ratio of elastic modulus $n_o = E_t/E_b$ and the power-law parameter p where n_o is changed in range of [1–20] and p is in range of [0–20]. The values of the correction coefficients for every couple (p, n_o) are captured in Table 1. It is noted that the shear correction factors k depend strongly on the values of p and specially n_o . Indeed, we see that the correction factors will decrease as n_o increases. They take the value $k = 5/6$ as the homogeneous plate for $p = 0$ or $n_o = 1$ and approximately this usual value for $p = 1$. Furthermore, it is higher than $5/6$ for $p < 1$. To consider the effect of changing the correction coefficients on the deflection of the plate, we consider firstly the value $k = 0.6595$ which corresponds to $p = 6$ and $E_t/E_b = 6$ (SiC, $E_t = 420$ GPa and Aluminum, $E_b = 70$ GPa) and $k = 0.576$ corresponds to $p = 7$, $E_t = 696$ GPa (Monotungsten carbide-WC), $E_b = 70$ GPa (Aluminum). The obtained deflection from these cases are used to compare with the deflection of the models using $k = 5/6$ and $k = 1$.

The measurement of “relative error” is defined by the relationship:

$$\text{error}(\%) = \frac{M_c - M_m}{M_m} \times 100\% \quad (23)$$

where M_m is the value obtained from the present model, and M_c the value obtained from other models.

TABLE 1
Shear correction factors

p	E_t/E_b									
	1	2	3	4	5	6	8	10	15	20
0	5/6	5/6	5/6	5/6	5/6	5/6	5/6	5/6	5/6	5/6
0.2	5/6	0.8396	0.8418	0.8429	0.8435	0.8440	0.8445	0.8448	0.8453	0.8455
0.4	5/6	0.8411	0.8439	0.8453	0.8462	0.8467	0.8474	0.8478	0.8483	0.8486
0.6	5/6	0.8396	0.8420	0.8433	0.8441	0.8446	0.8453	0.8457	0.8461	0.8463
0.8	5/6	0.8364	0.8374	0.8381	0.8386	0.8389	0.8395	0.8399	0.8404	0.8406
1.0	5/6	0.8320	0.8309	0.8305	0.8304	0.8305	0.8308	0.8312	0.8319	0.8323
2.0	5/6	0.8095	0.7924	0.7804	0.7720	0.7662	0.7593	0.7563	0.7555	0.7580
3.0	5/6	0.7961	0.7666	0.7433	0.7247	0.7099	0.6882	0.6738	0.6556	0.6498
4.0	5/6	0.7905	0.7547	0.7248	0.6997	0.6786	0.6451	0.6203	0.5810	0.5599
5.0	5/6	0.7891	0.7506	0.7175	0.6890	0.6643	0.6238	0.5923	0.5381	0.5046
6.0	5/6	0.7899	0.7507	0.7163	0.6861	0.6595	0.6150	0.5794	0.5158	0.4741
7.0	5/6	0.7917	0.7530	0.7183	0.6875	0.6600	0.6132	0.5751	0.5053	0.4581
8.0	5/6	0.7940	0.7563	0.7221	0.6912	0.6634	0.6155	0.5759	0.5020	0.4508
9.0	5/6	0.7964	0.7602	0.7267	0.6962	0.6685	0.6202	0.5799	0.5032	0.4492
10.0	5/6	0.7989	0.7642	0.7316	0.7017	0.6743	0.6262	0.5856	0.5073	0.4513
15.0	5/6	0.8090	0.7820	0.7551	0.7293	0.7048	0.6602	0.6210	0.5419	0.4823
20.0	5/6	0.8157	0.7947	0.7729	0.7511	0.7300	0.6902	0.6540	0.5780	0.5183

TABLE 2
Relative error of the non-dimensional deflection of the plate (w_{max}/h), WC-AI

a/h	$k_1 = k_2 = 1$	$k_1 = k_2 = 5/6$	$k_1 = k_2 = 0.576$	E_t/E_b	n
5	2.2177e-06 (−9.68%)	2.2823e-06 (−7.05%)	2.4554e-06	9.9426	7
10	3.1608e-05 (−2.92%)	3.1866e-05 (−2.13%)	3.2559e-05	9.9426	7
20	4.9023e-04 (−0.77%)	4.9126e-04 (−0.56%)	4.9403e-04	9.9426	7
50	0.018980 (−0.13%)	0.018986 (−0.091%)	0.01900	9.9426	7

Table 2 gives the relative error measurement of the non-dimensional maximum deflection in terms of the various side-thickness ratio of the plate for WC-AI FGM. Note that it is not the case which carries out the correction factors at least. It can be seen in this case that the variation of the correction factor does not affect the deflection of the FG plate for thin and medium-thick plates. That is due to the fact that contribution of the shear deformation energy is negligible compared to bending deformation energy. The influence is only visible for the thick plate ($a/h \leq 10$). However, the correction factors will become meaningful when the ratio of elastic modulus increases and thus its influence on the deflection can become more significant (about 11% for $n_o = 20$, $p = 8$, $a/h = 5$) as Figure 6. The difference of the deflection in this case also shows that shear forces in a one-layer Reissner-Mindlin FG plate did not affect the deformation of the plate. It could be more significant for the case of sandwich FG plates for which the stiffness of the medium part of the plate is significantly lower than the upper and lower parts of the plate.

Figure 7 represents the deflection at the center line ($x, y = b/2$) for various shear correction factors and Figure 8 presents a comparison between the results of different models. The three-dimensional finite element computation using Abaqus software with elements C3D8R, is performed by using a appropriate mesh

comprising 8 layers in the thickness direction. It can be seen that the deflection obtained from the present model is identical to the results of Abaqus three-dimensional finite element model and the higher-order shear deformation models (TSDT, SSDT). The difference between these results and the result obtained from the model using the shear correction factor $k = 5/6$ is approximately 5% for the case of SiC-AI FGM material (Figure 8). This deviation will become bigger as n_o increases (Figures 5 and 6). The variation of the plane stress σ_{xx} at the center of the FG plate along the thickness direction is depicted in Figure 9. It is compared with the models of Reddy (TSDT) [14] and Zenkour (SSDT) [19]. It is noted that, for the case of $p = 6$, the in-plane stresses of the FSDT model can be represented by a 7th order function of z and the transversal shear stresses have the form of the 8th order of z . We note that there is no significant difference of the membrane stress between the different models. There is only one small variation on the maximum compressive stress between the model of first order shear deformation and the models of higher order shear deformation.

Figure 10 presents the variation of the plane stress σ_{xx} at the center of the plate according to the various values of the power-law material parameter. It can be seen that the maximum compressive stress at the center of the FG plate is at the top

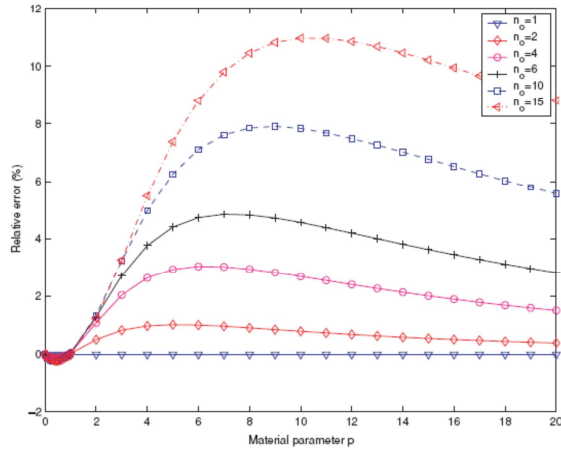


FIG. 5. Relative error of maximal deflection, $a/h = 5$.

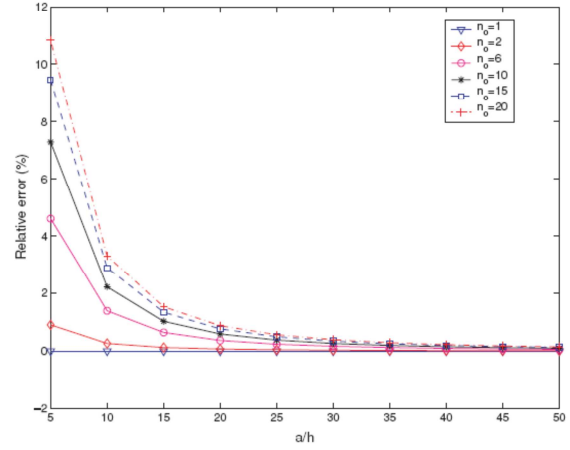


FIG. 6. Relative error of maximal deflection, $p = 8$.

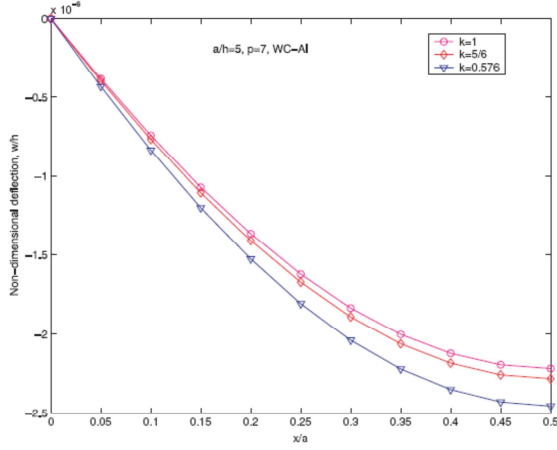


FIG. 7. Variation of deflection \bar{w} for the shear factors, WC-Al, $a/h = 5$, $p = 7$.

surface and increases as the material parameter p increases. In comparison, the maximum tensile stress is located inside the plate for $p < 1$. This is a significant difference compared to usual homogeneous composite laminate.

The transverse shear stress defined in (17) near the boundary edge ($x = 99a/100$, $y = 49b/100$) is compared to that of model admitting $k = 5/6$ and shown in Figure 11. As for the in-plane stress, no significant differences can be seen by its appearance. This can be explained due to the one-layer Reissner-Mindlin FG plate model, which carries out a negligible influence of the variation of the FGM material properties on the secondary variables. The shear stress within the plate given by the present model (FSDT) is now compared with the higher-order shear deformation models in which the shear stresses are obtained from the

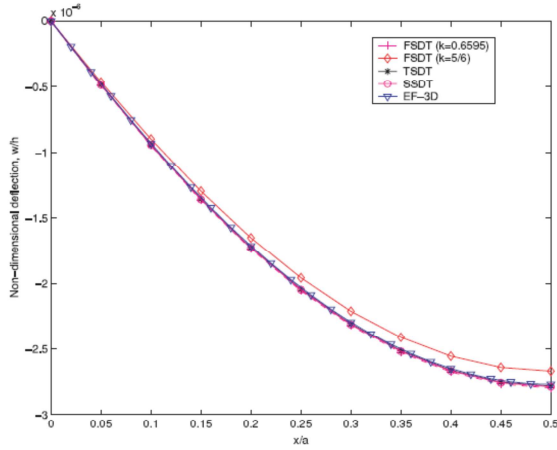


FIG. 8. \bar{w} for the models, $a/h = 5$, $p = 6$, SiC-Al.

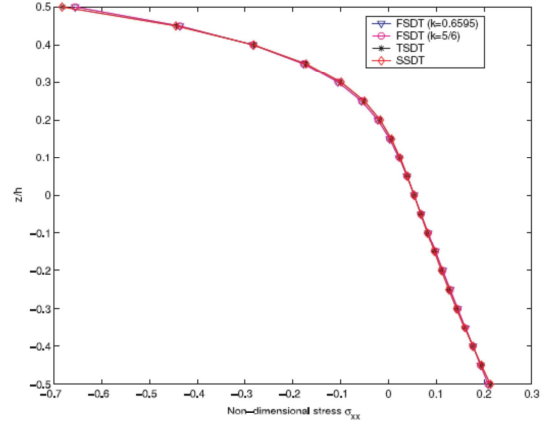


FIG. 9. Stress $\bar{\sigma}_{xx}$, $a/h = 5$, $p = 6$, SiC-Al.

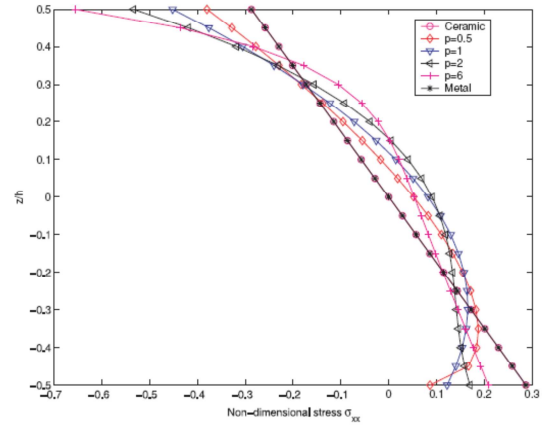


FIG. 10. Non-dimensional stress $\bar{\sigma}_{xx}$.

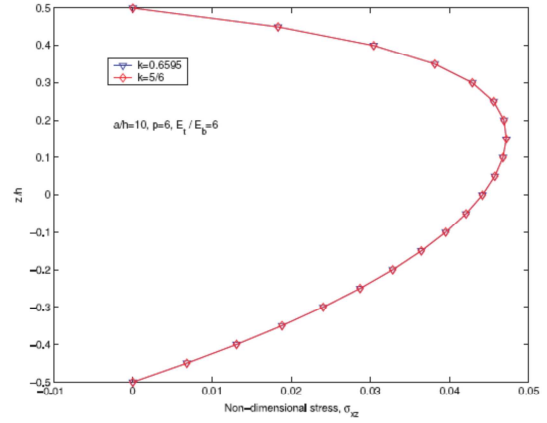


FIG. 11. Comparison of non-dimensional stress $\bar{\sigma}_{xz}$.

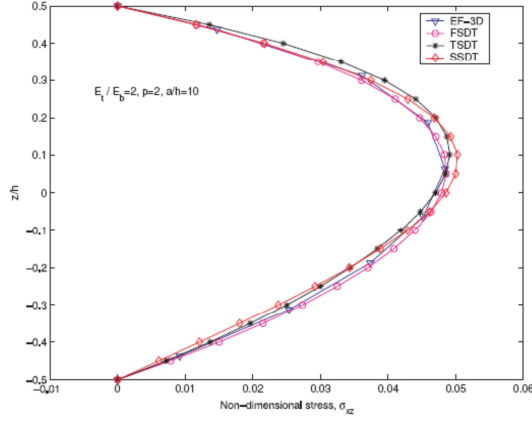


FIG. 12. Non-dimensional stress, $\bar{\sigma}_{xz}$.

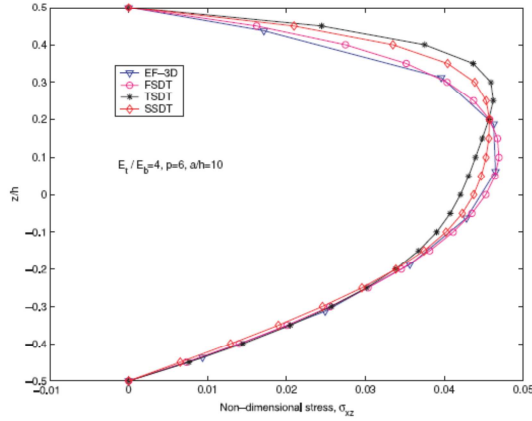


FIG. 13. Non-dimensional stress, $\bar{\sigma}_{xz}$.

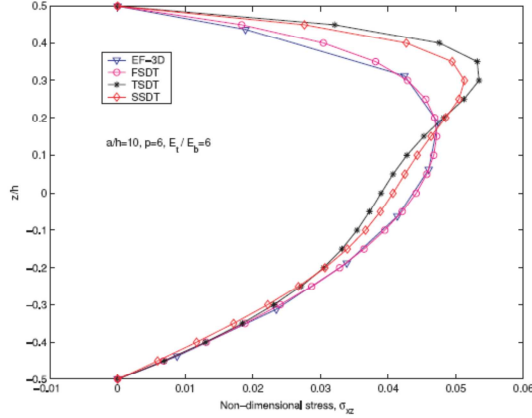


FIG. 14. Non-dimensional stress, $\bar{\sigma}_{xz}$.

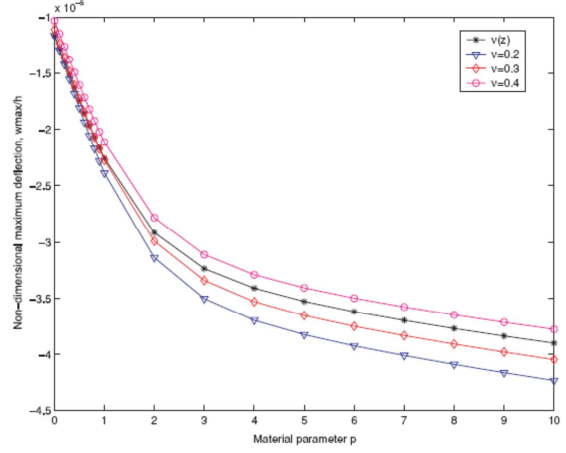


FIG. 15. Effect of Poisson's ratio on the maximum deflection, $a/h = 10$, $E_t/E_b = 6$.

constitutive law [11, 14, 19]. The variation of the shear stress near the boundary edge of the plate ($x = 99a/100$, $y = 49b/100$) through the plate thickness is represented in Figures 12, 13 and 14. We note that the shear stress of the FSDT model and the three-dimensional element finite model is nearly the same. In comparison with the higher-order models, it can be seen in this case that the curves are clearly different for the three models (FSDT, TSDT, SSDT). The relative difference between the values of shear stresses can reach 25% at some locations within the plate for ($n_o = 6$, $p = 6$). It also shows us that this distinction depends on the ratio of the Young's modulus and the material parameter. Indeed, the difference between the FSDT model and the higher-order models (TSDT, SSDT) is small for the small values of (n_o , p) (see Figure 12). Finally, the transversal stress of the present model is adapted with the three-dimensional finite element solution.

The results of the FG Reissner-Mindlin plate in the previous part is based under the assumption that the Poisson's ratio is constant. To investigate the effect due to this coefficient, a continuously graded Poisson's ratio through the thickness of the plate is considered, as given by relationship (3), with $\nu_t = 0.2$ and $\nu_b = 0.4$. The maximum deflection according to the variation of the material parameter thus obtained is shown in Figure 15. The results can be compared with those related to constant values of the Poisson's ratio and show that the deflection of the FG plate is affected by the variation of Poisson's ratio through the thickness of the plate for $p > 2$.

4. CONCLUSIONS

The improved shear stiffnesses and the shear correction coefficients for the functionally graded Reissner-Mindlin were presented. With this modification, the Navier's solution for a simply supported square FG plate based on the first-order shear

deformation (FSDT) was computed. The obtained results enable us to note that the shear correction factor is not the same for the FG plate as for a homogeneous plate and is a function of the material distribution, especially ratio of elastic moduli through the plate. However, this variation does not affect the stress fields of the Reissner-Mindlin FG plates. This correction is only effective on the deflection of thick plates and it can become remarkably for the medium-thick plates when the ceramic-metal elastic modulus's ratio is taken more than 10. The maximum tensile stress of the functionally graded plate is located within the plate, in opposition to the case of an homogenous plate. The variation of the shear stress through the thickness of the FG plate given by the FSDT model is however different from the variation given by higher order shear deformation models.

REFERENCES

- Koizumi, M., "FGM Activities in Japan." *Composites* **28**, 1-4 (1996).
- Suresh, S., and Mortensen, A., *Fundamentals of functionally graded materials: Processing and thermomechanical behavior of graded metals and metal-ceramic composites*. IOM Communication, London (1998).
- Kawasaki, A., and Wanatabe, R., "Concept and P/M Fabrication of Functionally Graded Materials." *Ceramics Int.* **23**, 73-83 (1997).
- Kieback, B., Neubrand, A., and Riedel, H., "Processing techniques for functionally graded materials." *Mat. Sci. Eng. A* **362**, 81-106 (2003).
- Chi, S., and Chung, Y., "Mechanical behavior of functionally graded material plates under transverse load - Part I: Analysis." *Int. J. Sol. Struc.* **43**, 3657-3674 (2006).
- Chi, S., and Chung, Y., "Mechanical behavior of functionally graded material plates under transverse load - Part II: Numerical results." *Int. J. Sol. Struc.* **43**, 3675-3691 (2006).
- He, X. Q., Ng, T. Y., Sivashankara, S., and Liew, K. M., "Active control of FGM plates with integrated piezoelectric sensors and actuators." *Int. J. Sol. Struc.* **38**, 1641-1655 (2001).
- Reissner, E., "The effect of transverse shear deformation on the bending of elastic plates." *J. Appl. Mech.* **13**, 69-77 (1945).
- Mindlin, R. D., "Influence of rotary inertia and shear on flexural motion of isotropic elastic plates." *J. Appl. Mech.* **18**, 31-38 (1951).
- Reddy, J. N., *Theory and Analysis of Elastic Plates*. Taylor Francis: Philadelphia (1999).
- Reddy, J. N., *Mechanics of Laminated Composites Plates: Theory and Analysis*. CRC Press: Boca Raton (1997).
- Praveen, G. N., and Reddy, J. N., "Nonlinear transient thermoelastic analysis of functionally graded ceramic-metal plates." *Int. J. Sol. Struc.* **35**, 4457-4476 (1998).
- Croce, L. D., and Venini, P., "Finite elements for functionally graded Reissner-Mindlin plates." *Computer Meth. in Appl. Mech. Eng.* **193**, 705-725 (2004).
- Reddy, J. N., "Analysis of functionally graded materials." *Int. J. Num. Meth. Eng.* **47**, 663-684 (2000).
- Cheng, Z. Q., and Batra, R. C., "Exact correspondence between eigenvalues of membranes and functionally graded simply supported polygonal plates." *J. Sound. Vibr.* **229**, 879-895 (2000).
- Ferreira, A. J. M., Batra, R. C., Roque, C. M. C., Qian and Martins, P. A. L. S., "Static analysis of functionally graded plates using third-order shear deformation theory and a meshless method." *Comp. Struc.* **193**, 705-725 (2004).
- Zenkour, A. M., "Buckling of fiber-reinforced viscoelastic composite plates using various plate theories." *J. Eng. Math.* **50**, 75-93 (2004).
- Zenkour, A. M., "Thermal effects on bending response of fiber-reinforced viscoelastic composite plates using a sinusoidal shear deformation theory." *Acta Mechanica* **171**, 171-187, (2004).
- Zenkour, A. M., "Generalized shear deformation theory for bending analysis of functionally graded materials." *Appl. Math. Modell.* **30**, 67-84 (2006).
- Cheng, Z. Q., and Batra, R. C., "Three-dimensional thermoelastic deformations of functionally graded elliptic plates." *J. Sound. Vibr.* **31**, 97-106 (2000).
- Ramirez, F., Paul, Heyliger, R., and Pan, E., "Static analysis of functionally graded elastic anisotropic plates using a discrete layer approach." *Composites, Part B: Engineering* **37**, 10-20 (2006).
- Vel, S., and Batra, R. C., "Exact solution for thermoelastic deformations of functionally graded thick rectangular plates." *AIAA Journal* **40**, (2002).
- Grujicic, M., and Zhang, Y., "Derivation of effective elastic properties of two-phase materials using Voronoi cell finite element method." *Mat. Sci. Eng. A* **251**, 64-76 (1998).
- Gasik, M. M., "Micromechanical modelling of functionally graded materials." *Compu. Mat. Sci.* **13**, 42-55 (1998).
- Timoshenko, S. P., and Woinowsky-Krieger, S., *Theory of Plates and Shells*. McGraw-Hill, New York (1959).
- Lee, K., and Lee, S. W., "A postprocessing approach to determine transverse stresses in geometrically nonlinear composite and sandwich structures." *J. Comp. Mat.* **37**, 2207-2224 (2003).
- Sze, K. Y., "Predictor-corrector procedures for analysis of laminated plates using standard Mindlin finite element models." *Comp. Struc.* **50**, 171-182 (2000).
- Zienkiewicz, O. C., and Zhu, J. Z., "The superconvergent patch recovery and a posteriori error estimates. Part I: The recovery technique." *Int. J. Num. Meth. Eng.* **33**, 1331-1364, (1992).
- Rolfes, R., Rohwer, K., and Ballerstaedt, M., "Efficient linear transverse normal stress analysis of layered composite plates." *Comput. Struc.* **68**, 643-652 (1998).
- Rolfes, R., and Rohwer, K., "Improved transverse shear stresses in composite finite elements based on first order shear deformation theory." *Int. J. Num. Meth. Eng.* **40**, 51-60 (1997).
- Caron, J. F., and Sab, K., "Un nouveau modèle de plaque multicouche épaisse." *Acad. Sci.* **329**, 595-600 (2001).
- Nguyen, V. T., Caron, J. F., and Sab, K., "A model for thick laminates and sandwich plates." *Comp. Sci. Tech.* **65**, 475-489 (2005).
- Noor, A. K., and Burton, W. S., "Assessment of shear deformation theories for multilayered composite plates." *Appl. Mech. Rev.* **42**, 1-13 (1989).
- Noor, A. K., and Burton, W. S., "Stress and free vibration analyses of multilayered composite plates." *Comp. Struct.* **11**, 183-204 (1989).
- Noor, A. K., and Burton, W. S., "Assessment of computational models for multilayered anisotropic plates." *Comp. Struct.* **14**, 233-265 (1990).
- Noor, A. K., Burton, W. S., and Peters, J. M., "Predictor-corrector procedure for stress and free vibration analyses of multilayered composite plates and shells." *Comput. Mech. Appl. Mech. Eng.* **82**, 341-364 (1990).
- Whitney, J. M., "Shear correction factors for orthotropic laminates under static load." *J. Appl. Mech.* **40**, 302-304 (1973).
- Vlachoutsis, S., "Shear correction factors for plates and shells." *Int. J. Num. Meth. Eng.* **33**, 1537-1552 (1992).
- Berthelot, J. M., *Matériaux Composites: Comportement Mécanique et Analyse des Structures*. Masson, Paris (1992).
- Nguyen, T. K., Sab, K., and Bonnet, G., "A Reissner-Mindlin model for functionally graded materials." *3rd European Conf. Compu. Mech.*, Lisbon (2006).